JMEPEG (2011) 20:1642–1647
DOI: 10.1007/s11665-011-9846-y

1059-9495/$19.00

Enhancement of Fatigue Properties of Ductile Irons by Successive Austempering Heat Treatment

M.R. Jahangiri, M. Nili Ahmadabadi, and H. Farhangi

(Submitted September 9, 2010; in revised form December 29, 2010)

The aim of this study is to evaluate the effects of austempering heat treatment on the microstructure, mechanical properties, and bending fatigue behavior of an alloyed ductile iron with chemical composition of 1.6 wt.% Ni, 0.47 wt.% manganese and 0.6 wt.% copper. Based on the results of tensile and impact tests, as well as metallographic studies, optimum heat-treating cycles were determined and applied on the standard fatigue specimens. The results showed that the fatigue strength of specimens austempered successively was practically comparable to those austempered at high temperatures and considerably greater than those austempered at low temperatures.

Keywords ADI, bainitic ferrite, fatigue behavior, successive austempering, toughness

1. Introduction

Austempered ductile iron (ADI) is an alloy with excellent mechanical properties that can be used instead of many different types of steel or aluminum alloys (Ref 1-4). Manufacturing process of components using this alloy consists of two steps of casting and subsequent heat-treating; each of them is essential to obtain the most appropriate quality. Austempering heat treatment of ductile irons includes austenitizing of cast parts in the temperature range of 875-950 °C for sufficient time followed by quenching in a molten salt bath or hot oil (Ref 5, 6). Austempering is performed over the temperature range of 230-450 °C according to the expected properties of the components. The holding time at the austempering temperatures depends on the various parameters and can be altered between 0.5 up to several hours. The effects of such heat treatments on the cast parts would be transforming the primary microstructure (austenite) to bainitic ferrite and remaining carbon-rich austenite (Ref 5-7). In fact, such a dual-phase microstructure will provide the desirable mechanical properties and permit steel or aluminum alloys to be replaced by ADI.

Although considerable amount of research has been done on fatigue behavior of ADI (Ref 8-15), some aspects of such behavior have not been examined. This is especially true for ductile irons which have been successively austempered. Since this type of heat treatment has provided satisfactory results (Ref 2, 16-19), it seems that the study of fatigue behavior of successive austempered alloys would provide positive results and valuable products.

The purpose of this study is to determine the optimum heat treatment cycles of conventional and two-step austempering treatments for an alloyed ductile iron and to investigate the fatigue behavior and mechanical properties of these ADIs.

M.R. Jahangiri, Metallurgy Department, Niroo Research Institute, Tehran, Iran; and **M. Nili Ahmadabadi** and **H. Farhangi**, Department of Metallurgy and Materials Engineering, University of Tehran, Tehran, Iran. Contact e-mail: mjahangiri@nri.ac.ir.

2. Experimental Procedure

Table 1 shows the chemical composition of ductile irons used in this study. To prepare the alloy, sorel pig, pure Ni, pure Cu, Fe-Si(75%), and Fe-Mn(75%) were melted in an induction furnace. The base iron melt was treated at 1500 °C by plunging method using ferrosilicomagnesium followed by inoculation with ferrosilicon before pouring. The pouring temperature was 1420 °C. Casting and solidification of Y-blocks was performed in green sand molds. Y block sizes were selected in according to ASTM: A897 Standard with leg dimensions of 25 mm. Impact, tensile, and fatigue specimens were prepared from Y block legs and after austempering they were tested and evaluated. Austenitizing temperature and time were 900 °C and 90 min, respectively. High and low temperature austempering were carried out at 375 and 235 °C, respectively, and for successive austempering, the specimens were initially heat-treated at 375 °C for 15, 30, or 60 min and then immediately at 235 °C. Time of the cycles was selected within 15 min to 12 h. In addition to the conventional mechanical properties and fatigue tests, some of the tensile and impact specimens were cut for metallographic studies and hardness measurements.

Fatigue tests were performed up to complete fracture of specimens or 10^7 cycles (some specimens were not broken until 10^7 cycles). Using this experimental data, *S-N* curves of alloy were obtained in different conditions of heat treatment. Frequency of tests was 12,000 cycles per minute and the applied cyclic stress was selected between 150 and 400 MPa.

3. Results and Discussion

3.1 Impact Strength

To determine the optimum heat treatment cycles of all austempering conditions, impact tests of the standard specimens were used. Since the impact resistance properties of an alloy indicate simultaneous strength and ductility properties, this is an easy method to determine the relative optimum conditions for these types of heat treatments.

Figure 1 shows the change in the absorbed energy of impact specimens which have been heat-treated according to different austempering cycles. In this figure, as well as the others, the specimens were coded according to the austempering heat treatment temperatures and times. For example, in specimen code 235(*t*), 235 stands for the austempering temperature in °C and *t* for the austempering time in minutes. In specimens austempered successively, the two stages of austempering heat treatment were coded, respectively.

The maximum absorbed impact energy is obtained in specimens subjected to high temperature austempering. This can be as a result of the presence of more retained austenite in the microstructure, absence of carbides in ferrite layers, or a lower dislocation density (Ref 1, 3, 4, 20, 21). Specimens austempered successively have intermediate levels of impact resistance and low temperature austempered alloys have the lowest impact toughness.

The processing window concept can be used to explain changes in mechanical properties and austenite stability over time of austempering in ADI alloys. In general, the austempering process is divided into two stages. In the first stage, primary austenite in the structure transforms to bainitic ferrite and carbon-rich austenite. At the end of this stage, there is a maximum amount of retained austenite phase in the structure. In the second stage, the existing austenite in the microstructure will start to decompose and carbide phases begin to form. Thus, a drop in impact resistance and ductility over time of austempering in ADI alloys is related to start of second stage reaction of austempering in which high-carbon austenite in the structure transforms to ferrite and carbide phases (Ref 19-21). The time interval between the first and the second stages is called heat treatment processing window (Fig. 2).

Table 1 Chemical composition of the alloy

Element	C	Si	Mn	Ni	Cu	Cr	Mo	Mg	P	S	Fe
wt.%	3.57	2.6	0.47	1.6	0.6	0.04	0.03	0.05	0.01	0.007	Bal.

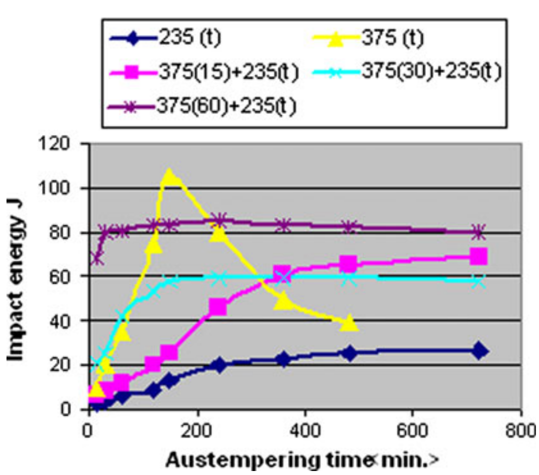

Fig. 1 Absorbed impact energy of various austempered specimens

As shown in Fig. 1, a sudden drop in the impact resistance takes place in specimens austempered at the high temperatures. The reason is the higher holding temperatures of these specimens in austempering treatments and, therefore, more time for the diffusion of carbon for reaching equilibrium and forming carbide phases. In low temperature and successive austempering cycles, such conditions have not happened.

3.2 Microstructure Studies

Microscopic studies showed that the specimens prepared from as-cast Y-blocks had a nodule count in the range of 90-120 graphite per mm^2 and the graphite nodularity was more than 80%. The microstructure of the as-cast ductile iron consisted of a bull's eye ferrite structure in pearlitic matrix and the amount of ferrite phase was about 15%.

Figures 3 and 4 show the microstructure of specimens austempered at different conditions. Figure 3 shows the differences of the austempering kinetics in the regions near or away from the graphite nodules. This is a result of segregation of carbide-forming elements and manganese in the intercellular regions of microstructure and their delaying effects on the austempering transformation (Ref 22-24).

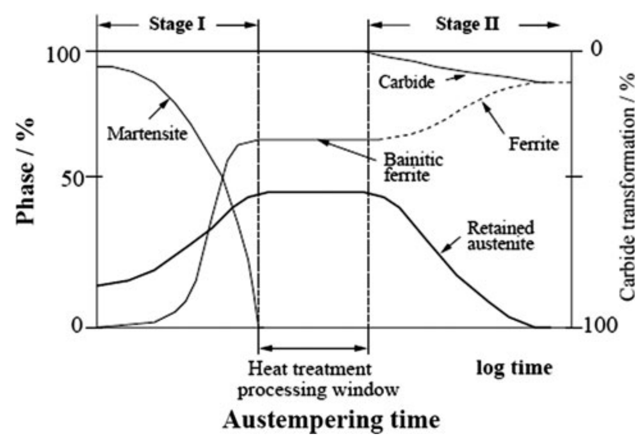

Fig. 2 Austempering processing window of ductile irons [5]

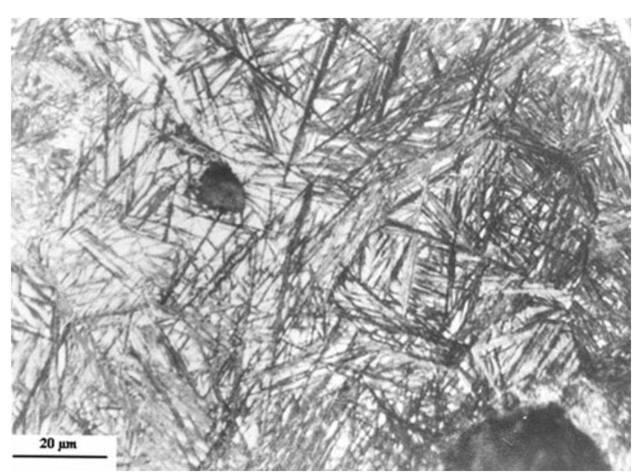

Fig. 3 Microstructure of alloys austempered at 235 °C for 8 h

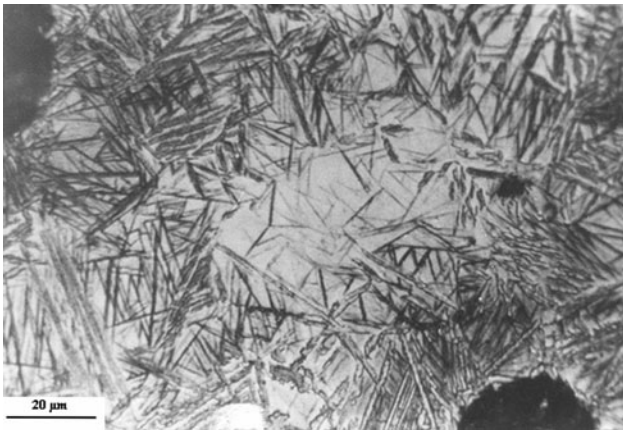

Fig. 4 Microstructure of alloys austempered successively (at 375 °C for 15 min. and immediately at 235 °C for 4 h)

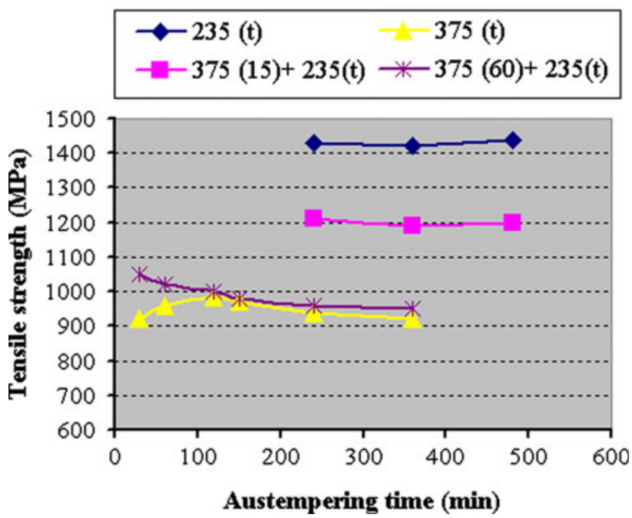

Fig. 5 Tensile strength of austempered specimens

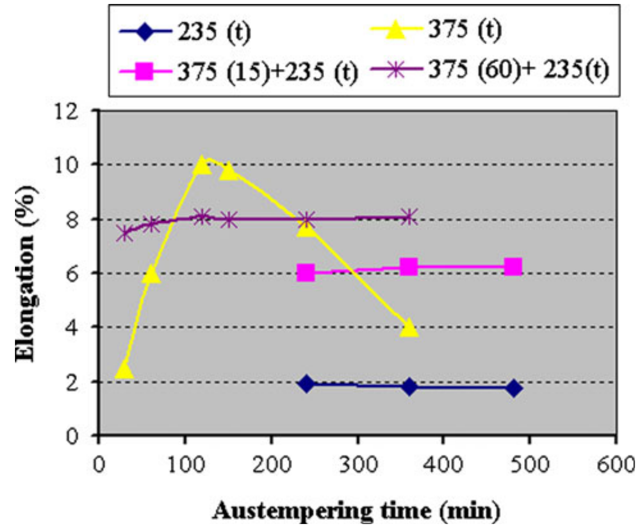

Fig. 6 Elongation of austempered specimens

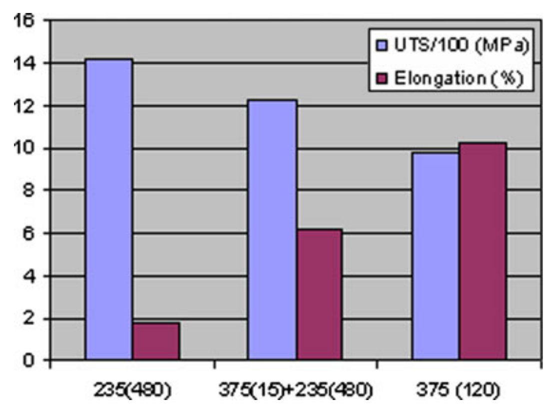

Fig. 7 Comparison of UTS vs. elongation for austempered specimens

The specimens heat-treated successively, have two types of upper and lower ausferrite microstructures simultaneously (Fig. 4). Upper ausferrite is generally formed adjacent to graphite nodules and lower ausferrite is often seen in intercellular regions (middle of Fig. 4). Authors predicted that these conditions could create an interesting condition, in which the properties of the successive austempered alloys could be controlled by various microstructures formed at different locations of the microstructure. In other words, in the alloys which are austempered successively, the properties controlled by the microstructure in the vicinity of the graphite nodules, are closer to alloys heat-treated isothermally at high temperatures and the properties controlled by the microstructure in the vicinity of the intercellular regions, are comparable to alloys heat treated isothermally at low temperatures.

3.3 Tensile Strength and Elongation

Figures 5 and 6 show strength and elongation properties of specimens austempered at different conditions. As indicated, the maximum tensile strength correlates to alloys heat-treated at low temperatures and fully transformed to lower ausferrite. Microstructure of such alloys is similar to Fig. 3 and consists of very fine ausferrite sheaves. The volume fraction of the retained austenite is very low in these microstructures. The presence of carbides and a high density of dislocations in these sheaves of fine ferrites makes such alloys very strong. Those samples heat-treated successively have more strength compared with the ones austempered at high temperatures.

Tensile elongation of the alloys austempered at different temperatures resulted in an inverse trend compared with the strength properties (Fig. 7). The reasons for variations of this property are the same as mentioned in the previous sections relating to the impact resistance of the alloys heat treated at different conditions. Figures 8 and 9 show SEM images of fracture surface of specimens heat-treated at different conditions. As can be seen, the specimens heat-treated at high temperatures show a ductile fracture surface and dimple coalescence is the main mechanism for fracture of such specimens. Ductile irons heat-treated successively show dual fracture features in a way that in some regions of the fracture surface (preferentially around graphite nodules), completely ductile characteristics can be seen, whereas in the other regions quasi cleavage fracture is dominant.

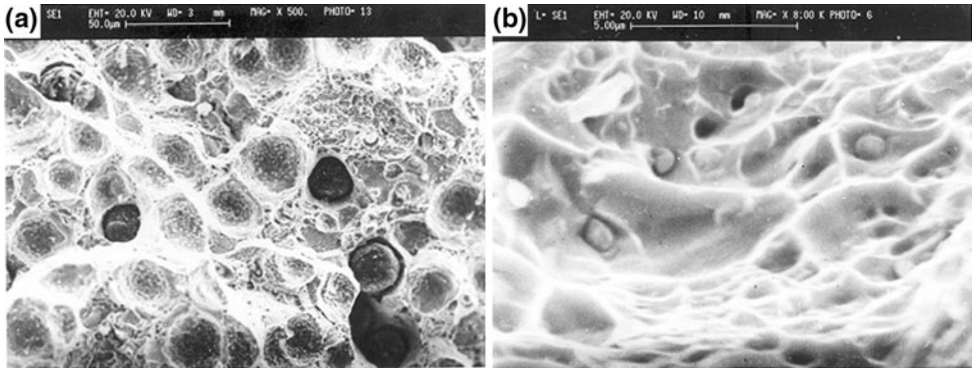

Fig. 8 SEM images of fracture surface of tensile specimen austempered at 375 °C for 2 h

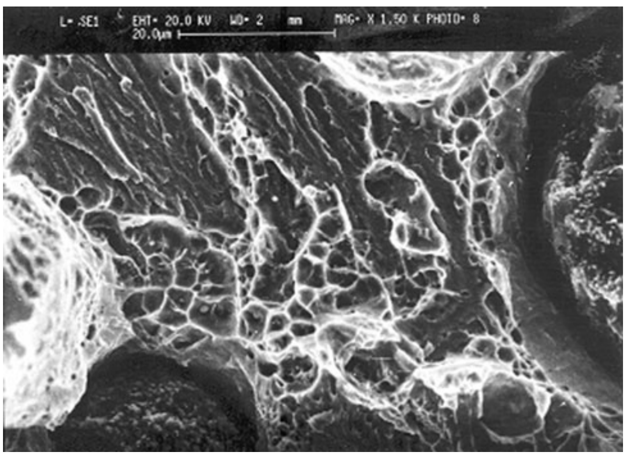

Fig. 9 SEM image of fracture surface of tensile specimen austempered successively (at 375 °C for 15 min. and immediately at 235 °C for 4 h)

3.4 Fatigue Behavior

Based on the results of impact, tensile and metallographic experiments, the optimum austempering cycles (times) for the alloy were determined as follows:

– High temperature heat treatment: 2 h at 375 °C.
– Low temperature heat treatment: 8 h at 235 °C.
– Successive heat treatment: 15 min at 375 °C and 8 h at 235 °C.

The optimum cycles refer to minimum austempering times at each temperature in which the impact and tensile properties reached maximum value. Figure 10 shows the fatigue behavior of the alloy after applying such heat-treating cycles to the standard fatigue specimens. As can be seen, for the three heat treatments, a fatigue limit can be defined below which fatigue life will be long. In general, the results in Fig. 10 show that the following relationship exists between the fatigue strength of the alloy and the heat treatment conditions:

Fatigue strength of the upper ausferrite
$\geq$ Fatigue strength of two-step structure
$\gg$ Fatigue strength of the lower ausferrite

According to the above results, the maximum fatigue strength of the alloy corresponds to the microstructures which

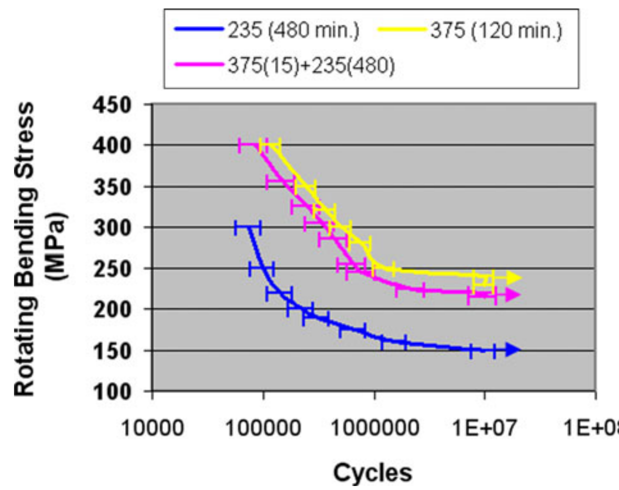

Fig. 10 *S-N* curves of austempered specimens

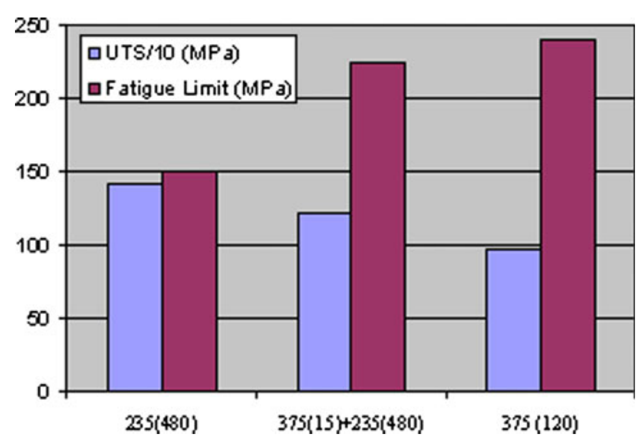

Fig. 11 Comparison of fatigue strength vs. tensile strength of various austempered specimens

have the lowest tensile strength and the highest impact toughness. This case which is in agreement with the results of other works (Ref 8-15, 25, 26) indicates that in ADIs, unlike conventional ferritic/pearlitic cast irons and steels, fatigue strength does not increase with increasing alloy strength (Fig. 11). On the other hand, this property increases with increasing toughness (Fig. 12) or amount of the retained austenite in the microstructure.

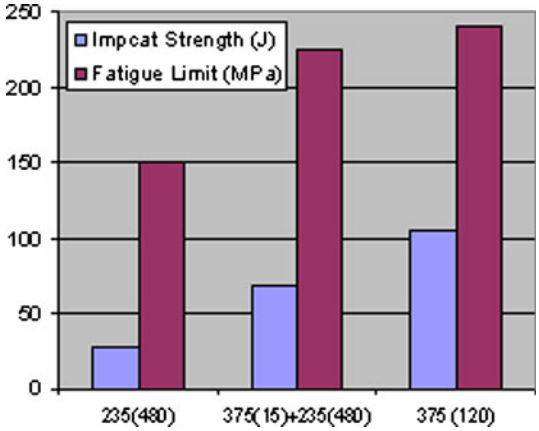

Fig. 12 Comparison of fatigue strength vs. impact strength for various austempered specimens

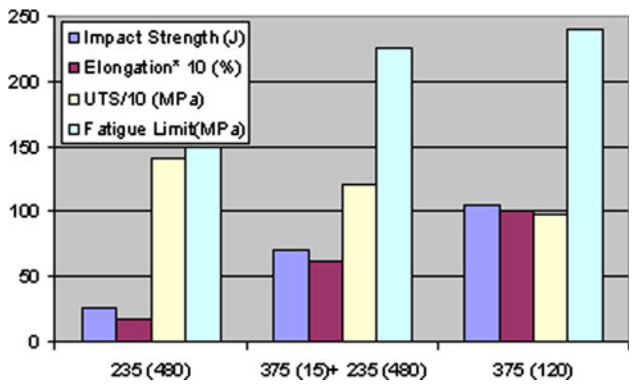

Fig. 13 Comparison of the main mechanical properties for various types of austempering cycles

The important point about the high-cycle fatigue behavior of successively austempered ADIs is that the fatigue strength of these specimens is comparable to those austempered at high temperatures and is very greater than those heat-treated at low temperatures. These results show that the main microstructural regions controlling the fatigue strength of the ADI are regions around the graphite nodules. These regions transform in the first stages of the austempering heat treatment. In the specimens austempered at the high temperatures or successively (2-step), these regions transform in the form of upper ausferrite which have more retained austenite and toughness. In the specimens transformed at the low temperatures, these fatigue life-controlling regions transform as lower ausferrite with very low toughness. Consequently, the fatigue life of such specimens will be much less than those austempered at the high temperatures or successively. It is necessary to note that upper and lower ausferrite may form in the both graphite adjacent and intercellular regions but the former forms mostly near to graphite nodules and vice versa.

3.5 Comprehensive Comparison of Properties

Figure 13 shows a comparison of the most important properties of the alloys austempered at different conditions. As shown, the alloys austempered successively are able to maintain their high strength along with the other main properties including impact resistance, ductility, and especially fatigue strength.

The upper-ausferrite ADIs exhibit higher impact strength (105 J), tensile elongation (10.2%) and fatigue limit (240 MPa) but lower tensile strength (980 MPa) than that of the lower-ausferrite ADIs (27 J, 1.95%, 150 and 1420 MPa). For successively austempered ductile irons, the higher impact strength (71 J), tensile elongation (6.2%), and fatigue limit (225 MPa) make these type of the ADIs to be better than the lower-ausferrite ADIs, while the higher tensile strength of these successively austempered alloys (1220 MPa) make them superior to the upper-ausferrite ADIs. These conditions can lead to extended applications of such heat treatment cycles in situations where it is necessary to have high fatigue strength properties in addition to impact toughness and tensile strength.

4. Conclusion

In this study, different effects of various austempering heat treatments have been studied on the microstructural, mechanical, and fatigue properties of ductile irons containing 3.57 wt.% C, 2.6 wt.% Si, 0.47 wt.% Mn, 1.6 wt.% Ni, and 0.6 wt.% Cu. On the basis of this study, it can be concluded that:

1. Austempering transformation temperature used for the investigated ductile iron is one of the important factors controlling transformation kinetics, microstructure, and mechanical properties.
2. Optimum properties of austempered specimens were obtained after 2 h at high temperature, after about 8 h at low temperature and for two-step specimens, after holding for 15 min at 375 °C and 8 h at 235 °C.
3. Despite the presence of a dual microstructure in ADI including bainitic ferrite and high carbon austenite, a specific quantity named fatigue limit can be obtained for the alloy.
4. Fatigue life of ductile irons austempered at high temperatures is much better than those austempered at low temperatures. This shows that there is no direct relationship between the tensile strength properties of ADIs and their fatigue strength.
5. Fatigue strength of ductile irons austempered successively is relatively equivalent to those austempered at high temperatures. The reason is proximity of remaining austenite (and toughness) in the regions of these ADIs microstructures which can control fatigue life of the alloy.

References

1. E. Dorazil, High Strength Austemperd Ductile Cast Iron, Horwood Series in Metals and Associated Materials, 1991
2. R.B. Gundlach and J. Janowak, Austempered Ductile Iron Combines Strength with Toughness and Ductility, *Met. Progr.*, 1985, p 19–26
3. R.A. Harding, The Production, Properties and Automotive Applications of Austempered Ductile Iron, *Kovove Mater.*, 2007, **45**(1), p 1–16
4. A. Polishetty, S. Singamneni, and G. Littlefair, "A Comparative Assessment of Austempered Ductile Iron as a Substitute in Weight Reduction Applications," ASME 2008 International Manufacturing Science and Engineering Conference, Vol 1, 2008, p 49–57
5. R.C. Voigt, Austempered Ductile Iron: Processing and Properties, *Cast Met.*, 1989, **2**(2), p 72–93
6. C.-H. Hsu and T.-L. Chuang, Influence of Stepped Austempering Process on the Fracture Toughness of Austempered Ductile Iron, *Metall. Mater. Trans. A*, 2001, **32**(10), p 2509–2514

7. A. Basso, M. Caldera, M. Chapetti, and J. Sikora, Mechanical Characterization of Dual Phase Austempered Ductile Iron, *ISIJ Int.*, 2010, **50**(2), p 302–306
8. K. Heyrynen et al., Tensile and Fatigue Properties of Relatively Pure ADI, AFS Trans, 1992, **100**, p 93–104
9. C.K. Lin et al., Influence of Microstructure on the Fatigue Properties of ADI: I—High Cycle Fatigue, *Int. J. Fatigue*, 1996, **18**(5), p 297–307
10. M. Bahmani, R. Elliott and N. Varahram, The Relationship Between Fatigue Strength and Microstructure in an Austempered Cu-Ni-Mn-Mo Alloyed Ductile Iron, *J. Mater. Sci.*, 1997, **32**(20), p 5383–5388
11. G.L. Greno, J.L. Otegui, and R.E. Boeri, Mechanisms of Fatigue Crack Growth in Austempered Ductile Iron, *Int. J. Fatigue*, 1999, **21**(1), p 35–43
12. J. Ortiz, A.P. Cisilino, and J.L. Otegui, Effect of Microcracking on the Micromechanics of Fatigue Crack Growth in Austempered Ductile Iron, *Fatigue Fract. Eng. Mater. Struct.*, 2001, **24**(9), p 591–605
13. J. Luo, R.A. Harding, and P. Bowen, Evaluation of the Fatigue Behavior of Ductile Irons with Various Matrix Microstructures, *Metall. Mater. Trans A*, 2002, **33**(12), p 3719–3730
14. S. Salman et al., Effect of Various Austempering Temperatures on Fatigue Properties in Ductile Iron, *Mater. Des.*, 2007, **28**(7), p 2210–2214
15. M.D. Chapetti, High-Cycle Fatigue of Austempered Ductile Iron (ADI), *Int. J. Fatigue*, 2007, **29**(5), p 860–868
16. M. Nili Ahmadabadi et al., Mechanical Properties of High Mn Ductile Iron Treated by Successive Austempering Process, *Trans. Jpn. Foun. Soc*, 1992, **11**, p 40–47
17. A.R. Ghaderi et al., Effect of Graphite Morphologies on the Tribological Behavior of Austempered Cast Iron, *Wear*, 2003, **255**(1–6), p 410–416
18. E.V. Pereloma and C.S. Anderson, Microstructure and Properties of Austempered Ductile Iron Subjected to Single and Two Step Processing, *Mater. Sci. Technol.*, 2006, **22**(9), p 1112–1118
19. A.H. Elsayed, M.M. Megahed, A.A. Sadek, and K.M. Abouelela, Fracture Toughness Characterization of Austempered Ductile Iron Produced Using Both Conventional and Two-Step Austempering Processes, *Mater. Des.*, 2009, **30**(6), p 1866–1877
20. K. Aslantas, I. Ucun, and K. Gok, Evaluation of the Performance of CBN Tools When Turning Austempered Ductile Iron Material, *J. Manufact. Sci. Eng.*, 2008, **130**(5), p 503–508
21. U. Batra, S. Ray, and S.R. Prabhakar, Impact Properties of Copper-Alloyed and Nickel-Copper Alloyed ADI, *J. Mater. Eng. Perform.*, 2007, **16**(4), p 485–489
22. B.Y. Lin, E.T. Chen, and T.S. Lei, The Effect of Segregation on the Austemper Transformation and Toughness of Ductile Irons, *J. Mater. Eng. Perform.*, 1998, **7**(3), p 407–419
23. M.N. Ahmadabadi and S. Farjami, Transformation Kinetics of Unalloyed and High Mn Austempered Ductile, *Mater. Sci. Technol.*, 2003, **19**(5), p 645–649
24. M. Erdogan, V. Kilicli, and B. Demir, Transformation Characteristics of Ductile Iron Austempered From Intercritical Austenitizing Temperature Ranges, *J. Mater. Sci.*, 2009, **44**(5), p 1394–1403
25. P. Shanmugam, P. Prasad Rao, K. Rajendra Udupa, and N. Venkataraman, Effect of Microstructure on the Fatigue Strength of an Austempered Ductile Iron, *J. Mater. Sci.*, 1994, **29**(18), p 4933–4940
26. M. Wohlfahrt, C. Oberwinkler, S. Tunzini, A. Rauscher, R. a Caballero, and W. Eichlseder, The Role of Sampling Position on Fatigue of Austempered Ductile Iron, *Procedia Eng.*, 2010, **2**(1), p 1337–1341